Static output feedback control for the rotation of a 2-DOF differential-algebraic quaternion camera

Maurício S. Richter, Aurélio T. Salton

School of Engineering, Universidade Federal do Rio Grande do Sul, Porto Alegre, RS (e-mail: {mauricio.richter,aurelio.salton}@ufrgs.br).

Abstract: This work proposes a static output feedback (SOF) image-based control design for a 2 Degree-of-Freedom (2-DOF) camera rotation with the objective of positioning an external feature at a desired projected display coordinate. Using a Differential-Algebraic Representation (DAR) of the nonlinear system to model the rigid-body dynamic equations in terms of quaternions, the Lyapunov stability analysis results in bilinear matrix inequalities (BMI) which are turned into an optimization problem subject to constraints. An algorithm that searches iteratively for the gain and the Lyapunov function coefficients by solving individual linear matrix inequalities (LMI) is used. Numerical examples are provided to evaluate the stabilization and performance results obtained with the proposed method.

Keywords: Nonlinear Systems, Visual-Based Rotation Control, Differential Algebraic Representation, Linear Matrix Inequalities, Static Output Feedback

1. INTRODUCTION

Rotational dynamic systems have a wide scope of applications, ranging from the aerospace sector, concerning attitude control for aircraft, quadrotors or spacecraft (Salton et al., 2017), to robotic manipulators (Saraiva, 2019). A variety of other applications is also possible, such as in vision-based systems, relating to camera orientation control, as studied by Hu et al. (2009).

One way of representing such systems is through rigid-body motion equations using, alternatively to regular Euler angle representation, quaternions. Considering that, this scheme was used to implement state feedback control in Salton et al. (2017) and Saraiva (2019), which served as a basis for the development of this work. Another possible approach is using output feedback for the control of rational nonlinear systems, such as in Castro (2019).

Having that in mind, the aim of this paper is to develop a vision-based control method for the rotation of a camera, with the objective of positioning the image projection of light emitting points (called features) on a desired coordinate of the display. The pinhole camera model is used for image formation (Hu et al. (2009)) and the control strategy is intended to find an optimal static output feedback (SOF) gain for the closed-loop system which stabilizes the system. In order to specify state-space models for the control design, this work focuses on a Differential-Algebraic Representation (DAR) of these nonlinear equations, as presented in Trofino and Dezuo (2014).

Using the image error as feedback, as well as the angular velocity, eliminates the need for sensing the angular position directly, which could increase the complexity and cost of the system. The controller to be designed, in addition to guaranteeing closed-loop asymptotic stability, maximizes the region of attraction of the system. The analysis and design problem is turned into BMI constraints, which are solved through an iterative optimization technique. Concerns with performance were taken regarding decay rate as well as oscillatory behavior of the closed-loop system.

⋆ This study was financed in part by the Coordenação deAperfeiçoamento de Pessoal de Nível Superior - Brasil (CAPES) -Finance Code 001 and by CNPq under Grant 306214/2018-0

2. PRELIMINARIES

In this work, the rigid-body rotation is expressed in terms of quaternions, which are hypercomplex numbers forming a four-dimensional real vector space $\mathbb{H}$ (Krishnaswami and Sachdev (2016)). A unit quaternion can then be defined as

$$q = \begin{bmatrix} \cos(\frac{\psi}{2}) \\ \boldsymbol{r}\sin(\frac{\psi}{2}) \end{bmatrix} = \begin{bmatrix} \eta \\ \epsilon \end{bmatrix} \tag{1}$$

where $\eta \in \mathbb{R}$, $\epsilon \in \mathbb{R}^3$, $\psi \in \mathbb{R}$ is the rotation angle $[rad]$ and $\boldsymbol{r} \in \mathbb{R}^3$ describes the rotation axis and its direction (by using the right-hand rule). From which it follows that,

$$\eta^2 + \epsilon^\intercal \epsilon = 1 \tag{2}$$

It is also necessary to define the following inertial frames:

Reference frame $\bar{\mathcal{F}}$: desired orientation of the camera, with $\bar{Z}$ pointing to the desired direction (with the feature at the desired position). Supposing one is "looking" towards $\bar{Z}$, $\bar{X}$ and $\bar{Y}$ are orthogonal axes, pointing to the right and up.

Body frame $\mathcal{F}$: camera frame, with the Z axis along a line on the direction the camera is pointing to, X to the right of the camera and Y pointing up.

A rotation matrix $R(q)$ in terms of a quaternion is defined as in Markley and Crassidis (2014):

$$R(q) = I - 2\eta S(\epsilon) + 2S(\epsilon)^2 \tag{3}$$

where $R(q) \in SO(3)$ and $S(\cdot)$ represents the cross-product in matrix form [1].

Given the above, the following result, Theorem 4.1 from Khalil (2002), will be used:

Lemma 1. Let $x = 0$ be an equilibrium point for $\dot{x} = f(x)$. Given a domain of interest $x \in \mathcal{X}$ containing the origin, if there is a Lyapunov candidate function $V(x) = x^\intercal P x$ such that

$$V(0) = 0,\ V(x) > 0 \ \text{ in } \ \mathcal{X} - \{0\} \tag{5}$$

$$\dot{V}(x) = x^\intercal P \dot{x} + \dot{x}^\intercal P x < 0 \ \text{ in } \ \mathcal{X} - \{0\} \tag{6}$$

Then $x = 0$ is an asymptotically stable equilibrium point and

$$\mathcal{R} = \{x : V(x) \leqslant 1\} \subset \mathcal{X} \tag{7}$$

is called a region of attraction, since every initial condition inside $\mathcal{R}$ asymptotically approaches the origin.

3. IMAGE FORMATION

This work uses the pinhole camera model (Ma et al., 2004), represented in Fig, 1, where both the feature μ and the projection m are shown. The projected coordinates are related to the external point as follows:

$$x = f\frac{\mu_x}{\mu_z} \qquad y = f\frac{\mu_y}{\mu_z} \tag{8}$$

where, $\mu = [\mu_x, \mu_y, \mu_z]$ are the coordinates of the feature, $[x, y]$ represent the position where the image plane is intersected and f is the focal length.

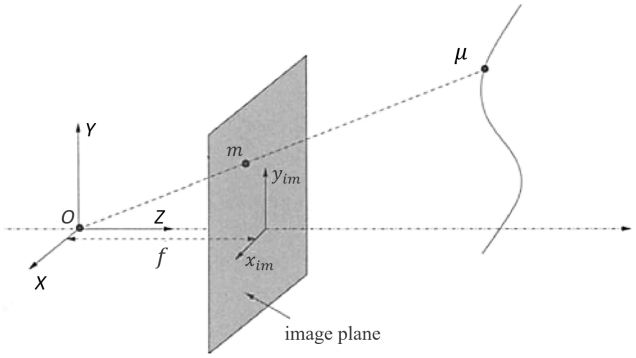

Figure 1. "Frontal" pinhole imaging model, adapted from Ma et al. (2004).

The resulting projection will be defined in terms of homogeneous coordinates, as defined in Graustein (1930):

Definition 3.1. Homogeneous Coordinates (x_1, x_2, x_3) of the finite point (x, y) are any three numbers x_1, x_2, x_3 for which

$$\frac{x_1}{x_3} = x, \qquad \frac{x_2}{x_3} = y \tag{9}$$

From Fig 1, by taking $\lambda = x_3$, a 2D point can be seen as the intersection of a line from the origin to the infinity with a plane spaced λ from the origin. If this depth is set to $\lambda = 1$, then $x_1 = x$ and $x_2 = y$ in (9). This system of coordinates facilitates transformations such as rotation and scaling using matrix operations, as such, the feature point is redefined as $\mu = [{}^{\mu_x}/_{\mu_z}\ {}^{\mu_y}/_{\mu_z}\ 1]^\intercal$.

From (8), considering the pixel scaling and translation to the display principal point, as well as the rotation to modify the reference of μ from the body frame to the reference frame, the image projection of a point can be set as in (Ma et al., 2004):

$$\lambda m = \underbrace{\begin{bmatrix} f_x & f_\theta & o_x \\ 0 & f_y & o_y \\ 0 & 0 & 1 \end{bmatrix}}_{K_c} R(q)\bar{\mu} \tag{10}$$

where $m = [x_{im}\ \ y_{im}\ \ 1]^\intercal$ establishes the image projection coordinates, $\lambda \in \mathbb{R}$ is the depth of the rotated point in relation to the camera frame, $\bar{\mu} \in \mathbb{R}^3$ is the desired point in relation to the reference frame and $K_c \in \mathbb{R}^{3\times3}$ is the intrinsic parameters matrix.

The intrinsic parameters concatenated in matrix K_c are dependent on the cameraparameters: $o_x, o_y \in \mathbb{R}$ - pixel coordinates of the principal point (image center); $f_x \in \mathbb{R}$: $f_x = \rho_x$ - where ρ_x is the size of unit length in horizontal pixels; $f_y \in \mathbb{R} : f_y = \frac{\rho_y}{\sin(\theta)}$ - where ρ_y is the size of unit length in vertical pixels and θ is the skew angle between camera axes; $f_\theta \in \mathbb{R} : f_\theta = -\rho_x \cot(\theta)$ - where ρ_x is the size of unit length in horizontal pixels and θ is the skew angle between camera axes.

4. MODEL AND REPRESENTATION

The rigid-body dynamic model in terms of quaternions can be described by (Markley and Crassidis (2014)):

$$\begin{cases} \dot{\eta} = -\dfrac{1}{2}\epsilon^\intercal \omega \\ \dot{\epsilon} = \dfrac{1}{2}\big(\eta I_3 + S(\epsilon)\big)\omega \\ J\dot{\omega} = -S(\omega)J\omega + \tau \end{cases} \tag{11}$$

where $\omega \in \mathbb{R}^3$ is the angular velocity $[rad/s]$, $J \in \mathbb{R}^{3x3}$ is the body moment of inertia $[kg \cdot m^2]$, $\tau \in \mathbb{R}^3$ is the input torque $[N \cdot m]$ and $S(\cdot)$ represents the cross-product in matrix form.

As described in Salton et al. (2017), since when imposing ϵ to a certain value, η is consequently a result of equation (2), then it is possible to eliminate η dynamic behavior equation from the model, resulting in the following state-space system:

$$\begin{cases} \dot{\epsilon} = \dfrac{1}{2}\big(\eta I_3 + S(\epsilon)\big)\omega \\ J\dot{\omega} = -S(\omega)J\omega + \tau \end{cases} \tag{12}$$

where the states are chosen as ϵ and ω. η, whose dynamic equation was removed, still appears on the state-space matrices and will be treated as an uncertainty with predefined limits.

As an output of the system, and serving as feedback, the image error is taken. It is defined as the difference between the current image and the desired image, in terms of pixels along each axis of the display, $\hat{X}_{im}$ and $\hat{Y}_{im}$.

Based on the feature image projection process described in Hu et al. (2009), let the vectors $\mu = [{}^{x}/_{z}\ {}^{y}/_{z}\ 1]^\intercal$ and $\bar{\mu} = [{}^{\bar{x}}/_{\bar{z}}\ {}^{\bar{x}}/_{\bar{z}}\ 1]^\intercal \triangleq [a\ b\ 1]^\intercal$ represent the current and

[1] In matrix form, the cross-product $\boldsymbol{x} \times \boldsymbol{y}$ can be expressed by:

$$S(\boldsymbol{x})\boldsymbol{y} = \begin{bmatrix} 0 & -x_3 & x_2 \\ x_3 & 0 & -x_1 \\ -x_2 & x_1 & 0 \end{bmatrix} \begin{bmatrix} y_1 \\ y_2 \\ y_3 \end{bmatrix} \tag{4}$$

desired feature's normalized coordinates in relation to the body frame and reference frame, respectively, so that,

$$\mu = \frac{\bar{z}}{z} R(q)\bar{\mu} = \gamma R(q)\bar{\mu} \tag{13}$$

Note that when the body frame is aligned with the reference frame, $R(q) = I_3$.

Since the feedback control law applied in this work is based on the image error, the scaling term γ in (13) is intentionally set to $\gamma = 1$ without loss of generality (Ma et al. (2004)). The image error, therefore, between the current projection m (rotated) and the desired projection $\bar{m}$ is defined by:

$$e = m - \bar{m} = K_c(R(q) - I_3)\bar{\mu} = K_c(-2\eta S(\epsilon) + 2S(\epsilon)^2)\bar{\mu} \tag{14}$$

Since the other output of the system is the state ω (rotation speed), acquired from an (inexpensive) gyroscopic sensor, the output of the system can be defined as:

$$y = \begin{bmatrix} e \\ \omega \end{bmatrix} \tag{15}$$

where $y \in \mathbb{R}^5$ is the output of the system, $e \in \mathbb{R}^2$ is the image error and $\omega \in \mathbb{R}^3$ is the rotation speed.

We will make use of the Differential Algebraic Representation (DAR), which consists in grouping the nonlinearities of the system in an additional vector $\xi(x)$ (or $\pi(x)$, whose terms are second or higher order groups of the states, as explained in Trofino and Dezuo (2014); Coutinho et al. (2004):

$$\begin{cases} \dot{x} = A_1(\eta)x + A_2\xi(x) + B_1\tau \\ 0 = \Omega_1(x)x + \Omega_2\xi(x) \\ y = C_1(\eta)x + C_2\pi(x) \\ 0 = \Pi_1(x)x + \Pi_2\pi(x) \end{cases} \tag{16}$$

where $x \in \mathbb{R}^n$ is the system state vector, $y \in \mathbb{R}^p$ is the output vector, $\xi \in \mathbb{R}^{n_\xi}$ is the nonlinear vector for the rigid-body dynamics and $\pi \in \mathbb{R}^{n_\pi}$ is the nonlinear vector for the output dynamics.

If Ω_2 is invertible, the original dynamics in (12) can be recovered by setting, as explained in Salton et al. (2017),

$$\dot{x} = \left(A_1(\eta) - A_2\Omega_2^{-1}(x)\right)x + B_1\tau \tag{17}$$

Letting, for the 2-dimensional model used,

$$x = \begin{bmatrix} \epsilon_x \\ \epsilon_y \\ \omega_x \\ \omega_y \end{bmatrix} \quad \xi = \begin{bmatrix} \epsilon_x\omega_y \\ \epsilon_y\omega_x \\ \omega_x\omega_y \end{bmatrix} \quad \pi = \begin{bmatrix} \epsilon_x^2 \\ \epsilon_y^2 \\ \epsilon_x\epsilon_y \end{bmatrix} \quad \tau = \begin{bmatrix} \tau_x \\ \tau_y \end{bmatrix}, \tag{18}$$

the resulting matrices are expressed by:

$$A_1 = \begin{bmatrix} & \frac{1}{2}\eta & 0 \\ 0_{2x2} & 0 & \frac{1}{2}\eta \\ & 0_{2x2} & \end{bmatrix} \quad A_2 = 0_{4x3} \quad B_1 = \begin{bmatrix} & 0_{2x2} & \\ j_x^{-1} & & 0 \\ 0 & & j_y^{-1} \end{bmatrix}$$

$$\Omega_1 = \begin{bmatrix} -\omega_y & 0 & 0 & 0 \\ 0 & -\omega_x & 0 & 0 \\ 0 & 0 & -\omega_y & 0 \end{bmatrix} \quad \Omega_2 = I_{3\times 3}$$

$$C_1 = \begin{bmatrix} 2(f_\theta\eta - o_x b\eta) & 2(o_x a\eta - f_x\eta) & 0 & 0 \\ 2(f_y\eta - o_y b\eta) & 2o_y a\eta & 0 & 0 \\ 0 & 0 & 1 & 0 \\ 0 & 0 & 0 & 1 \end{bmatrix}$$

$$C_2 = \begin{bmatrix} -2(o_x - f_\theta b) & -2(o_x - f_x a) & 2(f_\theta a + f_x b) \\ -2(o_y - f_y b) & -2o_y & 2f_y a \\ 0 & 0 & 0 \\ 0 & 0 & 0 \end{bmatrix}$$

$$\Pi_1 = \begin{bmatrix} -\epsilon_x & 0 & 0 & 0 \\ 0 & -\epsilon_y & 0 & 0 \\ -\epsilon_y & 0 & 0 & 0 \end{bmatrix} \quad \Pi_2 = I_{3\times 3} \tag{19}$$

5. CONTROL DESIGN

We sill now determine a static output feedback gain that maximizes the region of attraction such that every initial state in inside this region approaches the origin at a decay rate of at least σ.

Let $x_\epsilon \coloneqq \epsilon$ and $x_\omega \coloneqq \omega$ represent the state vectors for the quaternion and the rotation speed, respectively. $\mathcal{X}$ can then be defined as the domain of interest according to:

$$\mathcal{X} = \left\{ x_\epsilon \in \mathbb{R}^2, x_\omega \in \mathbb{R}^2 : \sum_i \frac{x_{\epsilon i}^2}{\alpha_i} + \sum_i \frac{x_{\omega i}^2}{\beta_i} \leq 1 \right\} \tag{20}$$

where $i = 1, 2$ and $\mathcal{X}$ forms a hyperellipsoid with α_i being the squared length limit for the i^{th} dimension of ϵ and β_i the squared length limit for the i^{th} dimension of ω.

The objective is to design a control law that maximizes $\mathcal{R} \subset \mathcal{X}$ in which the origin is asymptotically stable, which is equivalent to:

$$\left\{ x_\epsilon^\intercal M^{-1} x_\epsilon + x_\omega^\intercal N^{-1} x_\omega \leq 1 \right\}, \forall x : \; x^\intercal P x \leq 1, \tag{21}$$

where $M = diag(\alpha_i)$ and $N = diag(\beta_i)$, for $i = 1, 2$.

Applying the $\mathcal{S}$-procedure (Boyd and Vandenberghe (2004)):

$$\exists \kappa \in \mathbb{R}^+ : \left\{ \kappa P - \begin{bmatrix} M^{-1} & 0 \\ 0 & N^{-1} \end{bmatrix} \succeq 0 \right\} \tag{22}$$

which defining $\kappa = 1$ and using the Schur complement (Boyd and Vandenberghe (2004)) can be stated as the inequality (restriction to the optimization problem)

$$\begin{bmatrix} P & I_n \\ I_n & \Upsilon \end{bmatrix} \succeq 0, \text{ where } \Upsilon = \begin{bmatrix} M & 0 \\ 0 & N \end{bmatrix} \tag{23}$$

β_i limits are calculated dividing a desired angular range $\{\pm\psi_{\hat{X}}, \pm\psi_{\hat{Y}}\}$ on the image axes by an estimated settling time t_s. The criteria is relaxed with a low t_s so it only restricts the otherwise unbounded limits, although avoiding a constraint on the actual speed rotation of the camera.

These angular axes limits are translated into independent quaternions as

$$q_{\psi_x} = \begin{bmatrix} \cos(\frac{\psi_x}{2}) & 0 & \sin(\frac{\psi_x}{2}) & 0 \end{bmatrix}^\intercal, \quad q_{\psi_y} = \begin{bmatrix} \cos(\frac{\psi_y}{2}) & \sin(\frac{\psi_y}{2}) & 0 & 0 \end{bmatrix}^\intercal \tag{24}$$

where $(\psi_{\hat{X}})$ is associated with a rotation around the camera Y axis and $(\psi_{\hat{Y}})$ with a rotation around the camera X axis. With these values, the range for η and ϵ can then be set as

$$q_{lim} = \begin{bmatrix} \min\{\eta_{\psi_x}, \eta_{\psi_y}\} & 1 \\ -\epsilon_{\psi_y} & \epsilon_{\psi_y} \\ -\epsilon_{\psi_x} & \epsilon_{\psi_x} \\ 0 & 0 \end{bmatrix} \tag{25}$$

In a polytopic approach to evaluate the stability of the domain of interest (DoI), a convex hull of vertices containing the ellipsoid is defined so that $\mathcal{X} \subset \bar{\mathcal{X}} \subset \mathcal{V}_{\bar{\mathcal{X}}}$. Considering

the ellipsoid form of $\mathcal{X}$, the domain $\bar{\mathcal{X}}$ contained by the vertices $\mathcal{V}_{\bar{\mathcal{X}}}$ was defined as an octagon, as shown in figure 2, being less conservative on the region evaluated allowing a larger region of attraction to be found.

Based on q_{lim}:

$$\bar{\mathcal{X}} = \left\{ x \in \mathbb{R}^n : |x_1| \leq \epsilon_{\psi_y} \cos\phi_i,\ |x_2| \leq \epsilon_{\psi_x} \sin\phi_i \right\} \quad (26)$$

where $i = 1, \ldots, 8$, $\epsilon_{\psi_x}, \epsilon_{\psi_y}$ are obtained from (25), $\phi_1, \ldots, \phi_8$ are equally spaced angles from 0 to 2π rad and $\bar{\mathcal{X}} \subset \mathcal{V}_{\bar{\mathcal{X}}}$.

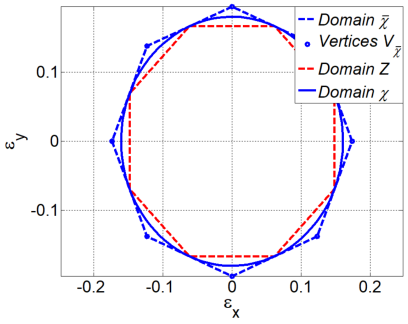

Figure 2. Forming the domain of interest.

Then, to delimit the DoI $\mathcal{X}$ inside $\bar{\mathcal{X}}$, a procedure adapted from Polcz et al. (2015) is done: new vertices $\mathcal{V}_{\mathcal{Z}}$ are defined as the average points of $\mathcal{V}_{\bar{\mathcal{X}}}$, resulting in an inner polytope $\mathcal{Z} \in \mathcal{V}_{\mathcal{Z}}$, shown in figure 2. Then, the domain of interest $\mathcal{X}$ is maximized within vertices $\mathcal{V}_{\mathcal{Z}}$ by finding:

OP1:

$$\max_{M,\upsilon} \upsilon : \begin{cases} M \succeq 0,\ \upsilon \geq 1 \\ \begin{bmatrix} z \\ 1 \end{bmatrix}^\intercal \begin{bmatrix} M & 0 \\ 0 & -\upsilon \end{bmatrix} \begin{bmatrix} z \\ 1 \end{bmatrix} \geq 0,\ \begin{bmatrix} z \\ 1 \end{bmatrix}^\intercal \begin{bmatrix} M & 0 \\ 0 & -1 \end{bmatrix} \begin{bmatrix} z \\ 1 \end{bmatrix} \leq 0 \end{cases} \quad (27)$$

where $M = \begin{bmatrix} \alpha_1 & 0 \\ 0 & \alpha_2 \end{bmatrix}$ is the matrix to be used in (23).

In addition to the parameters (x, η) which are inherently variables of the functions, the desired position of the feature in the image projection, represented by $\{a, b\}$, is also assigned to a range given upper and lower bounds. The following "uncertainties" $\Delta \subset \mathcal{V}_\Delta$ are defined:

$$\Delta = \left\{ \begin{array}{l} \delta_1 \coloneqq \eta : \min\{\eta_{\psi_x}, \eta_{\psi_y}\} \leq \delta_1 \leq 1 \\ \delta_2 \coloneqq a : |\delta_2| \leq \tan\psi_{\hat{Y}},\ \delta_3 \coloneqq b : |\delta_3| \leq \tan\psi_{\hat{X}} \\ \delta_4 \coloneqq a\eta : \underline{\delta_4} \leq \delta_4 \leq \bar{\delta_4},\ \delta_5 \coloneqq b\eta : \underline{\delta_5} \leq \delta_5 \leq \bar{\delta_5} \end{array} \right\} \quad (28)$$

where $\delta = [\delta_1\ \delta_2\ \delta_3\ \delta_4\ \delta_5]^\intercal$, $\{\eta_{\psi_x}, \eta_{\psi_y}\}$ are defined in (25), $\{\psi_{\hat{X}}, \psi_{\hat{Y}}\}$ are the desired angular range, $[\underline{\delta_4}, \bar{\delta_4}]$ are the minimum and maximum values of all combinations of $\delta_2\delta_1$, respectively, and $[\underline{\delta_5}, \bar{\delta_5}]$ are the minimum and maximum values of all combinations of $\delta_3\delta_1$, respectively. Finally, the camera intrinsic parameters $\{o_x, o_y, f_x, f_y, f_\theta\}$ and camera inertia parameters $\{j_x, j_y, j_z\}$ are considered constants.

5.1 Main Result

Given the domain of interest $\mathcal{X}$ in (20) and polytopes $\bar{\mathcal{X}}$ in (26) and Δ in (28), the following theorem, adapted from Coutinho et al. (2004); Salton et al. (2017); Saraiva (2019); Castro (2019), addresses the asymptotic stability with exponential performance and constrained oscillatory behavior of the closed-loop 2D DAR quaternion camera system.

Theorem 1. Considering the DAR representation (16) of system (12) and letting $u = Ky$ be the static output feedback control law for the closed-loop system: Suppose there are matrices $K \in \mathbb{R}^{m\times p}$, $Q = Q^\intercal \succeq 0 \in \mathbb{R}^{n\times n}$, $W_1 \in \mathbb{R}^{n_\xi \times n_\xi}$ and $W_2 \in \mathbb{R}^{n_\pi \times n_\pi}$ and positive scalars $\sigma \in \mathbb{R}, \nu \in \mathbb{R}$ such that for all (x, δ) evaluated at the convex set of vertices $\mathcal{V}_{\bar{\mathcal{X}}} \times \mathcal{V}_\Delta$:

$$\begin{bmatrix} \mathrm{He}\{FQ + \sigma Q\} & A_2(\delta)W_1^\intercal + Q\Omega_1^\intercal(x) & GW_2^\intercal + Q\Pi_1^\intercal(x) \\ \star & \mathrm{He}\{\Omega_2 W_1^\intercal\} & 0 \\ & & \mathrm{He}\{\Pi_2 W_2^\intercal\} \end{bmatrix} \prec 0 \quad (29)$$

$$\begin{bmatrix} Q & Q \\ Q & \Upsilon \end{bmatrix} \succeq 0 \quad (30)$$

$$\begin{bmatrix} -2\nu Q & FQ - (QF)^\intercal \\ -FQ + (QF)^\intercal & -2\nu Q \end{bmatrix} \prec 0 \quad (31)$$

where $F = A_1(\delta) + B_1KC_1(\delta)$ and $G = B_1KC_2(\delta)$.

Then, all closed-loop trajectories starting in $\mathcal{R}$ asymptotically approach the origin at a decay rate of at least σ with oscillation constrained by ν in the imaginary part of the eigenvalues of F, being this region of attraction defined as:

$$\mathcal{R} = \{x \in \mathbb{R}^n : x^\intercal P x \leq 1\} \subset \mathcal{X} \quad (32)$$

where $P = Q^{-1}$.

Proof. Considering a Lyapunov candidate function $V(x) = x^\intercal P x$, with $P = Q^{-1}$, the assumption taken that Q is a symmetric positive matrix leads to the conclusion that the function is positive definite. Then, in order to verify that (29) implies $\dot{V}(x) < 0$, first the dynamic of x is recalled from the DAR model in (16) taking into account the control law $\tau = Ky$, so that (dependence on (x, δ) is omitted from the proof):

$$\dot{x} = A_1 x + A_2 \xi + B_1 K C_1 x + B_1 K C_2 \pi \quad (33)$$

The derivative of $V(x)$ then becomes for the DAR:

$$\dot{V}(x) = \mathrm{He}\{x^\intercal P A_1 x + x^\intercal P B_1 K C_1 x + x^\intercal P A_2 \xi + x^\intercal P B_1 K C_2 \pi\} \quad (34)$$

By defining a vector $\zeta = [x^\intercal\ \xi^\intercal\ \pi^\intercal]^\intercal$, in a similar manner as Salton et al. (2017), it is possible to convert (6) it into the matrix inequality that follows:

$$\zeta^\intercal \begin{bmatrix} \mathrm{He}\{PA_1 + PB_1KC_1\} & PA_2 & PB_1KC_2 \\ A_2^\intercal P & 0 & 0 \\ C_2^\intercal K^\intercal B_1^\intercal P & 0 & 0 \end{bmatrix} \zeta < 0 \quad (35)$$

After that, by adding the decay rate term σ to (6):

$$\dot{V}(x) + 2\sigma V(x) < 0 \Leftrightarrow \dot{V}(x) < -2\sigma V(x) \quad (36)$$

being the result of this differential inequality, which guarantees the exponential decay rate:

$$V(x(t)) < V(x(0))e^{-2\sigma t}, \forall x(0) \in \mathcal{R} \quad (37)$$

From (36), the algebraic equations of the DAR are introduced in the stability problem, together with some scaling variables aiming to reduce conservatism of the results, as explained in Trofino and Dezuo (2014), and consequently the region of attraction. To achieve this, Finsler's Lemma (Boyd et al. (1994)) is applied thus obtaining:

$$\dot{V}(x) + 2\sigma V(x) + \mathrm{He}\left\{\xi L_1 [\Omega_1\ \Omega_2\ 0]\zeta\right\} + \mathrm{He}\left\{\pi L_2 [\Pi_1\ 0\ \Pi_2]\zeta\right\} < 0 \quad (38)$$

which is equivalent to (36) considering $[\Omega_1 \ \ \Omega_2 \ \ 0]\,\zeta = 0$ and $[\Pi_1 \ \ 0 \ \ \Pi_2]\,\zeta = 0$ according to the model representation defined in (16), and similarly to (35) turns into the following matrix inequality:

$$\begin{bmatrix} \mathrm{He}\{PA_1 + PB_1KC_1 + \sigma P\} & PA_2 + \Omega_1^\intercal L_1^\intercal & PB_1KC_2 + \Pi_1^\intercal L_2^\intercal \\ A_2^\intercal P + L_1\Omega_1 & \mathrm{He}\{L_1\Omega_2\} & 0 \\ C_2^\intercal K^\intercal B_1^\intercal P + L_2\Pi_1 & 0 & \mathrm{He}\{L_2\Pi_2\} \end{bmatrix} < 0 \tag{39}$$

By pre and post-multiplying (39) by $diag(Q, W_1, W_2)$ and its transpose, respectively, where $W_1 = L_1^{-1}$ and $W_2 = L_2^{-1}$, it finally results in (29).

The region of attraction of the system can be shown to be constrained to the elliptic range defined by $\mathcal{X}$, as stated in (32), in case (30) implies (21). The process described leading from the definition of the domain of interest in (20) to the inequality (23) is used and therefore it suffices to take the Schur complement (Boyd and Vandenberghe (2004)) and show that (30) can be written as:

$$Q - Q\Upsilon^{-1}Q \succeq 0 \tag{40}$$

which by pre and post-multiplying by P and applying again the Schur complement is equivalent to (23).

The constrained oscillation of the dynamic behavior of the system response is achieved by restricting the eigenvalues of $F = A_1(\delta) + B_1KC_1(\delta)$ to a horizontal band with limits on the imaginary part at $[-\nu, \nu]$.

The additional restriction (31) is the LMI condition for F to be $\mathcal{D}$-stable, that is, it ensures the eigenvalues of $F = A_1(\delta) + B_1KC_1(\delta)$ lie in a specified domain.

If (29)-(31) are satisfied for all vertices $\mathcal{V}_{\bar{\mathcal{X}}} \times \mathcal{V}_\Delta$, by convexity it can be assumed that it is true $\forall x \in \mathcal{X}$, $\forall \delta \in \Delta$ and consequently $\forall x \in \mathcal{R}$.

5.2 Optimization

To solve the SOF asymptotic stability problem, the optimization objective function focuses on minimizing the trace of $P = Q^{-1}$ for a fixed K, then minimizing the absolute value of the trace of the resulting matrix on the left side of (29) for a fixed $P = Q^{-1}$, with K as a variable. This second step is intended to maximize $\dot{V}(x)$ (negative) such that the system is still asymptotically stable, further enlarging the stability limits of the region of attraction.

An initial value for the gain K is obtained through a linearized model on the form, similar to a Quasi-LPV modeling (Huang and Jadbabaie (1999)),

$$\begin{cases} \dot{x} = A(x, \eta)x + B\tau \\ y = C(x, \eta)x \end{cases} \tag{41}$$

evaluated at the equilibrium point at the center of the image, with the desired feature at the same position, *i.e.*,

$$q_{eq} = \begin{bmatrix} 1 \\ 0 \\ 0 \\ 0 \end{bmatrix} \qquad \omega_{eq} = \begin{bmatrix} 0 \\ 0 \\ 0 \end{bmatrix} \qquad \bar{\mu}_{eq} = \begin{bmatrix} 0 \\ 0 \\ 1 \end{bmatrix} \tag{42}$$

Then, evaluating $\dot{V}(x) = xP\dot{x} + \dot{x}Px < 0$ with linearized $\dot{x} = Ax + BKCx$ and substituting $Z \in \mathbb{R}^{m\times n} : Z = KCQ$, with $Q = P^{-1}$, the following optimization problem, adapted from Salton et al. (2017), is solved:

$$\min_{Q,\,Z,\,N} \mathrm{trace}(N) : \begin{cases} AQ + QA^\intercal + BZ + Z^\intercal B^\intercal \prec 0 \\ \begin{bmatrix} Q & I \\ I & N \end{bmatrix} \succeq 0 \end{cases} \tag{43}$$

where $N = N^\intercal \in \mathbb{R}^{n\times n}$.

Using the Schur complement (Boyd and Vandenberghe (2004)), the bottom line of (43) implies $N \succeq Q^{-1} = P$, implicitly maximizing $\mathcal{R}$ since $\mathrm{trace}(N) > \mathrm{trace}(P)$. Then, in case the linearized state matrix C is invertible:

$$K_{init} = ZPC^{-1} \tag{44}$$

With that, it is possible to initialize the P-K algorithm with $K = K_{init}$. As a resulting optimization problem, with the objective of maximizing the region of attraction, the auxiliary decision variable $N = N^\intercal \in \mathbb{R}^{n\times n}$ is again defined, considering $\mathrm{trace}(N) > \mathrm{trace}(P)$, to solve:

OP1 (fixed K):

$$\min_{Q,W_1,W_2,N} \mathrm{trace}(N) : \begin{cases} (29), (30), (31), \forall x \in \mathcal{V}_{\bar{\mathcal{X}}}, \forall \delta \in \mathcal{V}_\Delta \\ \begin{bmatrix} Q & I \\ I & N \end{bmatrix} \succeq 0 \end{cases} \tag{45}$$

OP2 (fixed P):

$$\min_{K,W_1,N} |\mathrm{trace}(\Lambda)| : \begin{cases} (29), (31), \ \forall x \in \mathcal{V}_{\bar{\mathcal{X}}}, \ \forall \delta \in \mathcal{V}_\Delta \\ \begin{bmatrix} Q & I \\ I & N \end{bmatrix} \succeq 0 \end{cases} \tag{46}$$

where Λ is the resulting matrix on the left side of (29).

6. NUMERICAL RESULTS

To verify the control design, numerical results are presented in this section, with simulations performed in Matlab. Yalmip toolbox was used for the optimization problems (Lofberg (2004)), with solvers SDPT3 and SEDUMI.

The following constant parameters were set: camera intrinsic parameters and its moment of inertia as

$$K_c = \begin{bmatrix} 1244.4 & 0 & 640 \\ 0 & 1493.3 & 512 \\ 0 & 0 & 1 \end{bmatrix} \qquad J = \begin{bmatrix} 1 & 0 & 0 \\ 0 & 1 & 0 \\ 0 & 0 & 1 \end{bmatrix} \tag{47}$$

focal distance $f = 35mm$, standard resolution of $1280 \times 1024px$, Camera field of view (FOV) of $54.432° \times 37.849°$.

The optimization input parameters were set as:

$$\begin{cases} \psi_{\tilde{X}_{im}} = 26°, \ \psi_{\tilde{Y}_{im}} = 18.5°, \ \sigma = 0.25, \ \nu = 2rad/s \\ \text{Feature projection:} \quad \begin{matrix} \text{Initial:} & m_{init} = 250 \times 800px \\ \text{Desired:} & \bar{m} = 640 \times 512px \end{matrix} \end{cases} \tag{48}$$

As shown in figure 3, the algorithm finds a feasible solution in iteration 2, providing a valid trace of P. This trace is minimized as expected along the 10 iterations performed with $\mathrm{trace}(P)_{10} = 77.3$, which, as presented in figure 4, results in a RoA (projected on the image in green, according to (10)) close to the DoI defined (in solid blue).

Next figures show results for quaternion $\{\epsilon_x, \epsilon_y\}$ and rotation speed $\{\omega_x, \omega_y\}$ along time in 8 seconds of simulation, as well as the image error norm, which approaches zero.

The feature image projection path from the initial to the desired position is shown in figure 8.

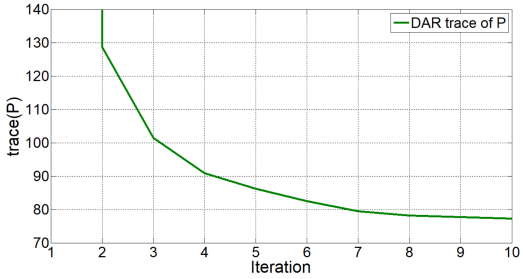

Figure 3. Trace of P along algorithm iterations.

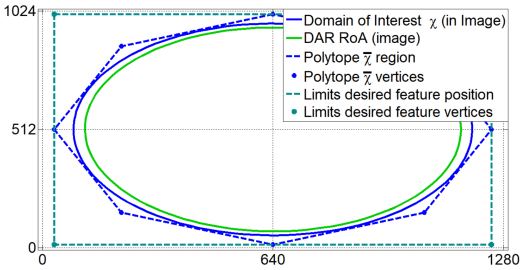

Figure 4. Region of attraction x Domain of interest.

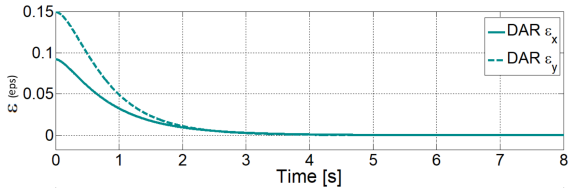

Figure 5. Quaternion ϵ along time.

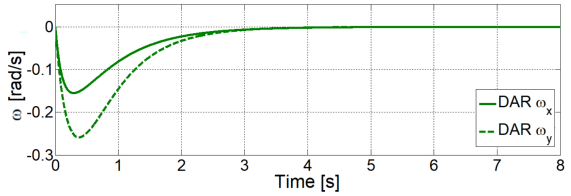

Figure 6. Rotation speed ω along time.

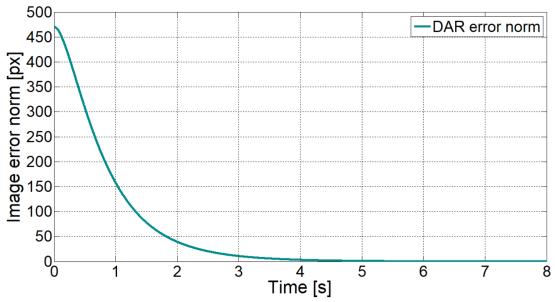

Figure 7. Image error norm along time.

7. CONCLUSION

Making use of a 2D DAR representation of a nonlinear quaternion camera rotation model, the problem of positioning a feature projection at a desired display coordinate, under constrained exponential decay and oscillation, was solved by finding an SOF controller that guarantees asymptotic stability by means of a P-K algorithm. The authors are investigating extensions to the 3D model.

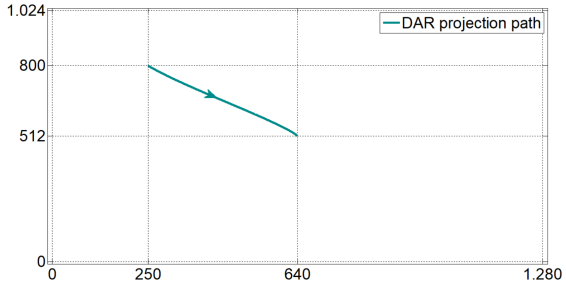

Figure 8. Image projection path.

REFERENCES

Boyd, S., El Ghaoui, L., Feron, E., and Balakrishnan, V. (1994). *Linear Matrix Inequalities in System and Control Theory*. SIAM, Philadelphia, PA.

Boyd, S. and Vandenberghe, L. (2004). *Convex Optimization*. Cambridge University Press, Cambridge, UK.

Castro, R.d.S. (2019). *Output Regulation of Rational Nonlinear Systems with Input Saturation*. Ph.D. thesis, UFRGS, Porto Alegre.

Coutinho, D.F., Bazanella, A.S., Trofino, A., and Silva, A.S. (2004). Stability analysis and control of a class of differential-algebraic nonlinear systems. *International Journal of Robust and Nonlinear Control*, 14(16), 1301–1326.

Graustein, W.C. (1930). *Introduction to Higher Geometry*. A series of mathematical texts. The Macmillan Company, New York.

Hu, G., Gans, N., Fitz-Coy, N., and Dixon, W. (2009). Adaptive homography-based visual servo tracking control via a quaternion formulation. *IEEE Transactions on Control Systems Technology*, 18(1), 128–135.

Huang, Y. and Jadbabaie, A. (1999). Nonlinear h control: An enhanced quasi-lpv approach. *IFAC Proceedings Volumes*, 32(2), 2754–2759.

Khalil, H.K. (2002). *Nonlinear Systems*. Prentice Hall, New Jersey, 3 edition.

Krishnaswami, G.S. and Sachdev, S. (2016). Algebra and geometry of hamilton's quaternions. *Resonance*, 21(6), 529–544.

Lofberg, J. (2004). Yalmip: A toolbox for modeling and optimization in matlab. In *2004 IEEE ICRA*, 284–289.

Ma, Y., Soatto, S., Kosecka, J., and Sastry, S.S. (2004). *An Invitation to 3-D Vision*. Springer-Verlag.

Markley, F.L. and Crassidis, J.L. (2014). *Fundamentals of spacecraft attitude determination and control*. Springer.

Polcz, P., Szederkényi, G., and Péni, T. (2015). An improved method for estimating the domain of attraction of nonlinear systems containing rational functions. In *Journal of Physics: Conference Series*, volume 659, 012038. IOP Publishing, Bristol, UK.

Salton, A.T., Castro, R.S., Borges, B.S., Flores, J.V., and Coutinho, D.F. (2017). Semidefinite programming solution to the spacecraft analysis and control problem. *IFAC-PapersOnLine*, 50(1), 3959–3964.

Saraiva, E.S. (2019). *Control design for robotic manipulator systems subject to saturating actuators*. Master's thesis, Pontifícia Universidade Católica/RS.

Trofino, A. and Dezuo, T. (2014). Lmi stability conditions for uncertain rational nonlinear systems. *International Journal of Robust and Nonlinear Control*, 24(18), 3124–3169.